Microstructure, Performance and Phase Study on T250 Maraging aging steel Pipe after Spinning and Aging

Caihong Chen[1, a], Shaoyu Zhang[1, b] and Yong'an Min[1, c]

[1]School of Materials Science and Engineering, Shanghai University, Shanghai 200072, China

[a]shucch@yeah.net, [b]1332066927@qq.com, [c]mya@staff.shu.edu.cn

Keywords: Maraging aging steels, Spinning, Aging, Microstructure, Performance, Phase.
Abstract. The raw material of tested T250 Maraging aging steel is solid-solution steel pipe. Microstructure, performance and phase changes of T250 steel pipe after spinning and aging were studied by Optical Microscope (OM), Scanning Electron Microscope (SEM), X-ray Diffraction (XRD), Three Dimensional Atom Probe (3DAP) tests and so on. The study shows that the structure of T250 is elongated and directional after spinning processing, and the matrix structure is martensite matrix with a large amount of global phases in diffuse distribution. After aging treatment, phases Al_3Ti and Ni_3Al transform into $Ni_3(Al,Ti)$ which gradually turns from globular to short rod, and Fe_2Mo to $MoSi_2$. The hardness of T250 steel pipe enhances mainly because of work hardening and aging strengthening.

Introduction

Developed by International Nickle Corporation (INCO) at the beginning of 1960s, Maraging aging steel is a kind of high alloy ultra-high strength steel with carbonless (or ultra-low carbon) iron-nickel martensite as matrix which has high specific strength and high fracture toughness because of precipitation and hardening of intermetallic compounds after aging [1]. The structure of T250 under solid-solution state is low-carbon martensite almost without work hardening, and no softening process is required in spinning. Featured with good performance in cold and heat treatment, good welding performance, and simple heat treatment process [2], maraging aging steel is widely applied in aviation and aerospace, marine, molding, and many other high-tech fields.

T250 steel is a kind of new-type maraging aging steel developed successfully in recent two decades. Without Co component, its cost is lower than the maraging aging steel with corresponding level of Co, while the mechanical property is similar [3]. This creates a good condition for enlarging the application of this material in cutting-edge technological fields. At present, T250 steel has been localized with continuous development. As maraging aging steel has good performance in cold deformation and processing, spinning is always applied to molding of thin-walled and high pressure resistant components [4]. Currently, the studies on localized T250 steel, especially studies on the structure and performance of thin-walled component after spinning and aging have not been mature and improved because more attention is paid to technology for heating processing. Moreover, most studies on T250 steel are in confidential.

This work explored mechanism of microstructure and phase changes in materials under different conditions of heat treatment by comparing structures, morphology, phases, and hardness of spinning T250 samples before and after aging processing. Therefore, we can realize effective control on microstructure and performance of T250 steel and improving study system.

Experimental

Materials. Materials used in this test is T250 steel pipe smelted by double-vacuum melting of "vacuum induced melting + vacuum self-consumption arc remelting" with wall thickness of 2.54mm and inner diameter of 69mm. Table 1 shows chemical components. Test materials have two states: (1) spinning state without aging; and (2) spinning with aging.

Methods. The solid solution treatment progress of T250 steel pipe is 820˚C.×1.5h. Then, thin-walled cylinder with 0.58mm wall thickness and constant inner diameter was processed by spinning. Spinning samples are aged for 4 hours at 460˚C., 500˚C., and 560˚C., respectively.

© 2015. The authors - Published by Atlantis Press

Samples after aging should take hardness test in MH-3 micro-sclerometer with 300 loading after removing oxidized surface by mechanical polishing. Microstructure was observed by Nikon MA100 OM; morphology was observed by SUPRA-40 field emission SEM with high resolution; phase analysis was conducted by D/max-rC XRD. The samples of 3DAP were taken with fine wire with cross section side length of 0.5mm and length of 30mm to do electrochemical polishing. After that, data are collected in LEAP 3000HR 3DAP, and analyzed with poSAP software.

Table 1 Compositions of T250 Maraging aging steel [wt. %]

C	Cr	Ni	Mn	Si	Mo	Ti	Al	P	S	Cu
≤0.01	≤0.50	18.00 ~ 20.00	≤0.10	≤0.10	2.75 ~ 3.25	1.20 ~ 1.60	0.05 ~ 0.15	≤0.008	≤0.005	≤0.50

Results

Hardness. Fig. 1 shows microhardness of T250 steel under different states. Compared with the hardness of spinning state, which is only 338.4HV, the hardness after aging obviously increases. With the rise of aging temperature, the hardness increases, and the sample at 500˚C. close to the peak aging state can reach relatively high hardness, 592.2HV. After peak aging, the hardness will gradually decrease with the rise of temperature. The sample at 560˚C. is in overaging state with hardness decreasing to 510.1HV.

Microstructure. Observed by OM, the matrix structure of spinning T250 samples is martensite which is tenuous and directional because of stress. Fig. 2 shows the microstructure of spinning T250 sample after aging at 560˚C.. The matrix structure is still martensite after spinning and aging. Compared with spinning structure, the overall morphology has no large change, but the structure refines and grain interior shows sign of precipitation to make the substructure richer.

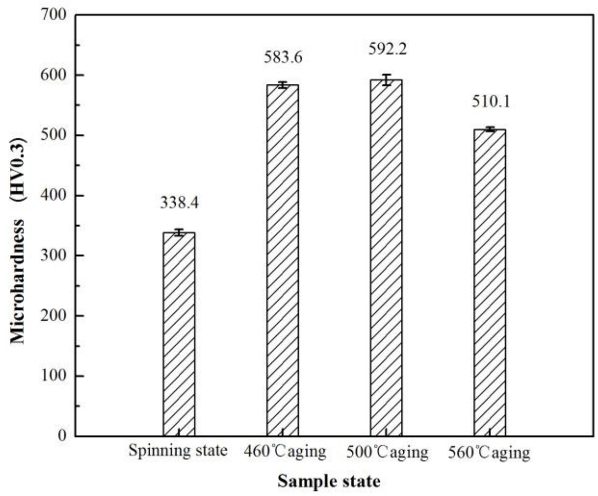

Fig. 1 Test results of microhardness of T250 samples in spinning state and after aging at 460˚C., 500˚C., 560˚C.

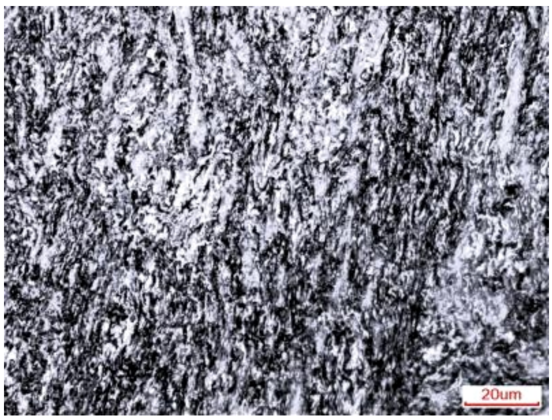

Fig. 2 Microstructure of spinning T250 sample after aging at 560˚C., magnification times 500×

Morphology. There are a lot of second phases in diffuse distribution at martensite lath boundary and inside of lath in spinning structure of T250 steel. The second-phase particles are mainly in globular shape with different sizes. There are a few large particles in size of about (200-400) nm which are distributed in partial location with relative concentrated distribution. There are also a large amount of small particles in size of about (5-50) nm which are distributed in the whole SEM view field relatively uniform, as shown in Fig. 3. Some second-phase particles are combined together.

EDS analysis is conducted in “1#” and “2#” microcells in Fig. 3-a. Table 2 shows the chemical components. “1#” microcell is the particle cell with higher Mo, Ti, and C content, but lower Fe and Ni content than matrix. It is deduced that globular large particles may be rich-Mo phase.

After the aging, a large amount of strengthening phases in different sizes and shapes, including globular, spherical, and short-rod particles are dispersively precipitated from martensite matrix as shown in Fig. 4. Compared with spinning state, the large particles after aging reduce. In addition, a lot of short-rod particles are precipitated from aging sample matrix. It can be found in comparison of SEM morphology of aging samples under different temperatures that with the rise of temperature, there are more and more second phases, and the particle morphology also changes.

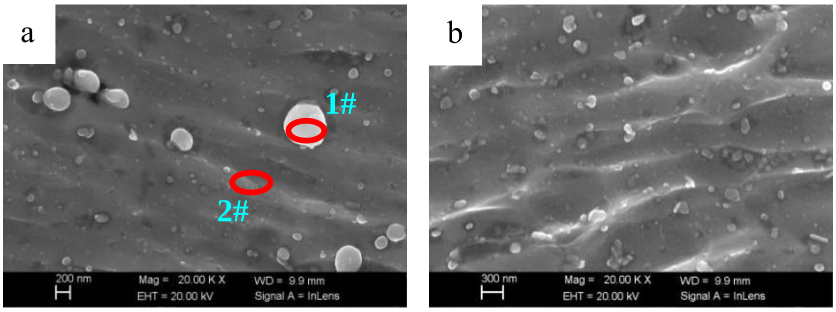

Fig. 3 SEM morphology of spinning T250 samples, magnification times 20000×

Table 2 Percentage of elements obtained in EDS analysis in two microcells of spinning T250 sample [wt. %]

Microcell	Fe	C	Mo	Ti	Ni	Cr
"1#", particle cell	40.3	28.6	17.3	5.3	8.0	0.4
"2#", matrix cell	66.3	9.8	4.8	2.1	16.5	0.4

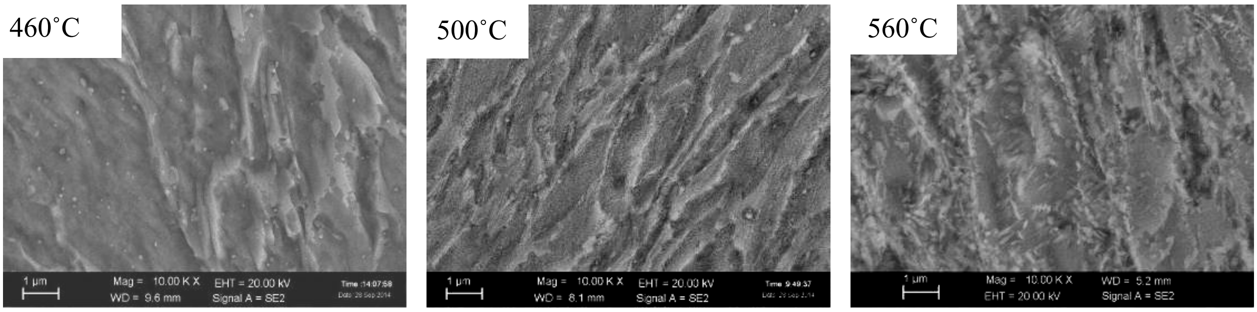

Fig. 4 SEM morphology of spinning T250 samples after aging at 460˚C., 500˚C., 560˚C., magnification times 10000×

Phase. Fig. 5 is XRD spectrum of T250 steel in spinning state and after aging under different temperatures. XRD spectrum of spinning T250 sample shows the existence of diffraction peaks of martensite, $Ni_3(Al,Ti)$, Fe_2Mo, Al_3Ti, $MoSi_2$, and Ni_3Al. After aging, the types of second phases keep unchanged, but the strength of diffraction peaks of $Ni_3(Al,Ti)$ and $MoSi_2$ significantly increases, while the strength of diffraction peaks of Fe_2Mo, Al_3Ti, and Ni_3Al decreases. This may be result from that aging makes phases Al_3Ti and Ni_3Al turn to $Ni_3(Al,Ti)$, and phase Fe_2Mo to $MoSi_2$.

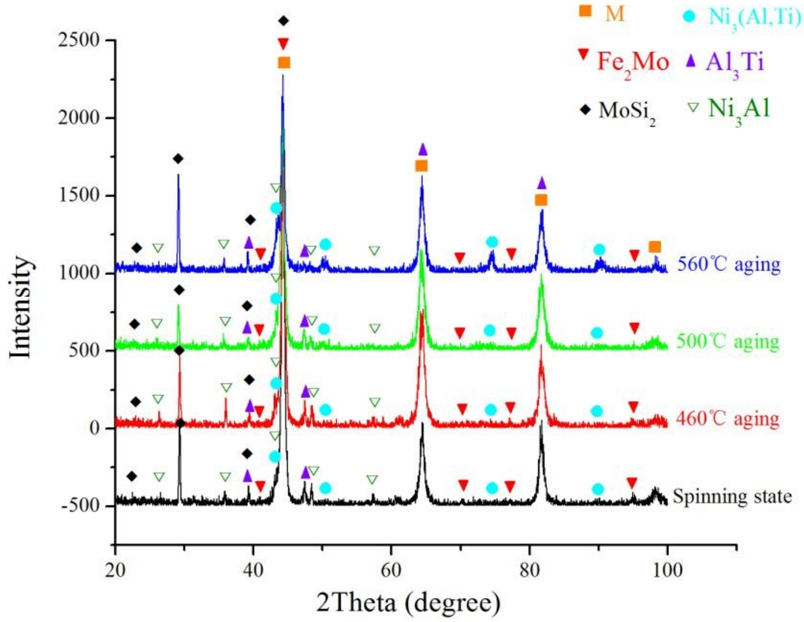

Fig. 5 XRD spectrum of spinning T250 sample and samples after aging at 460˚C., 500˚C., 560˚C.

Atomic arrangement. Fig. 6 shows the 3-dimensional distribution of atoms in major elements, including Fe, Mo, Ni, Ti, Al, and Cr in spinning sample, in which the 3-dimensional cube size is 30×30×75 nm. It can be seen that the atomic distribution is uniform.

Fig. 7 shows the 3-dimensional arrangement of atoms in all elements in aging samples, in which the 3-dimensional cube size is 50×50×75 nm. Fig. 7-c and 7-i show that Mo and Si atoms have segregation in the same position of 3-dimensional space. Fig. 7-d, 7-e, and 7-f show that Ni, Ti, and Al atoms have segregation in the same position of 3-dimensional space in strip shape. Cr and Mn atoms distribute evenly.

In order to further determine the phase, isoconcentration covers are made in segregation position of Mn and Si as shown in Fig. 8 with appropriate value of concentration according to average atom content. It can verify that Mo and Si segregate in the same position. Similarly, isoconcentration covers are made in segregation position of Ni, Ti, and Al as shown in Fig. 9. It can verify that Ni, Ti, and Al segregate in the same position. Therefore, there are phases $MoSi_2$ and $Ni_3(Al,Ti)$ in aging samples, and phase $Ni_3(Al,Ti)$ is precipitated in strip shape.

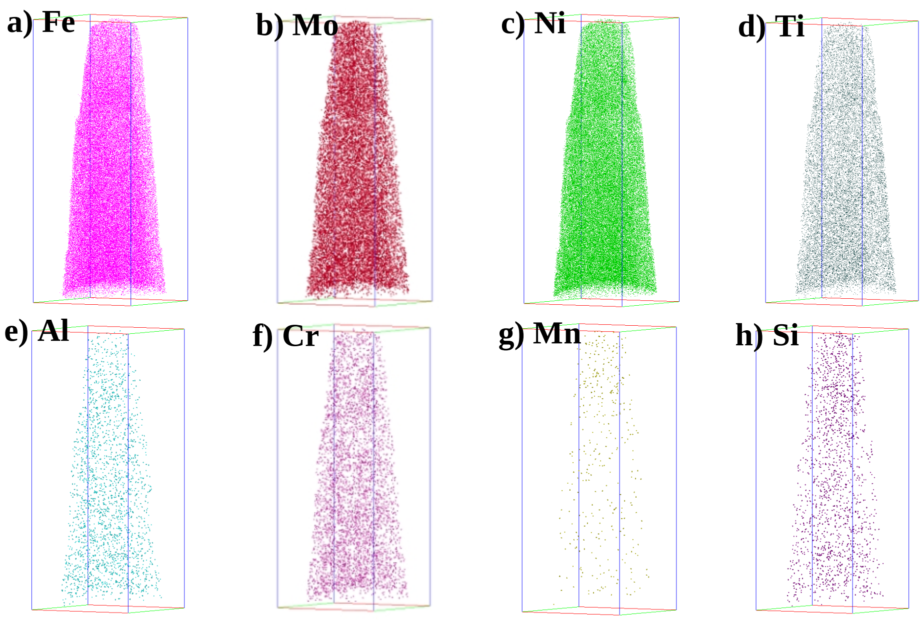

Fig. 6 Three dimensional distribution of major elements atoms in spinning samples

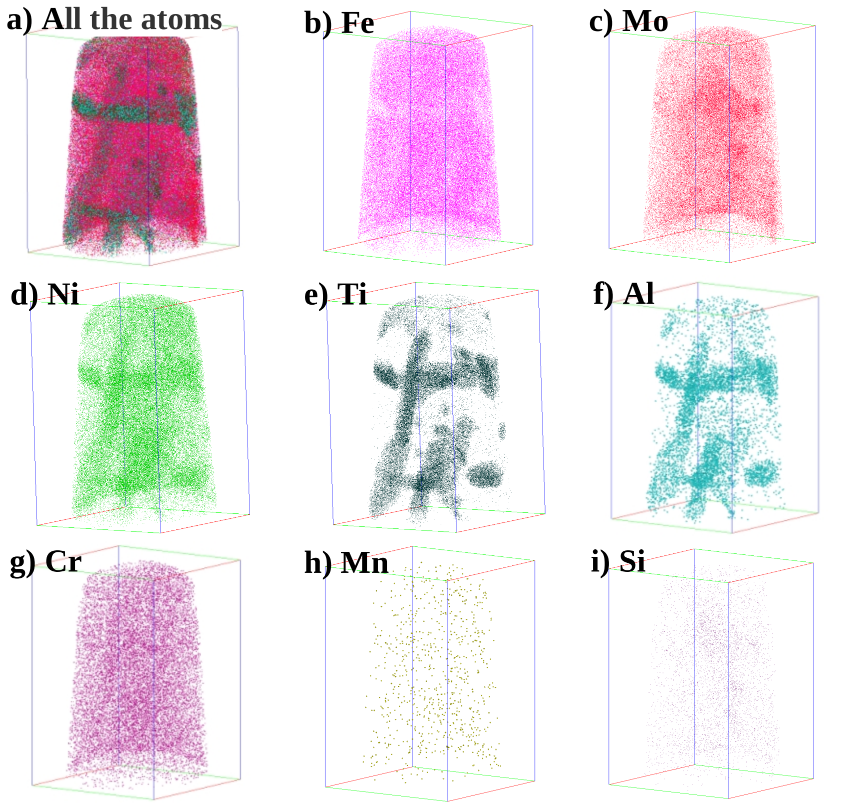

Fig. 7 Three dimensional distribution of
a) all element atoms and b-i) major element atoms in aging samples

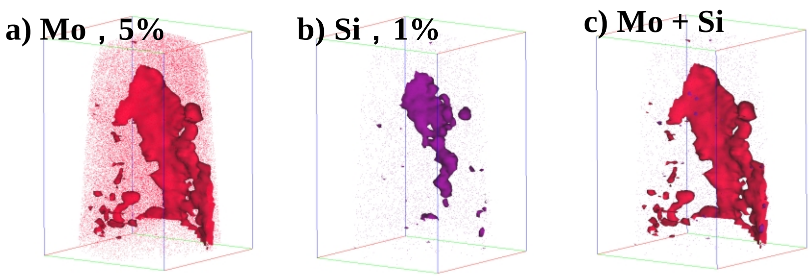

Fig. 8 Isoconcentration covers of Mn and Si

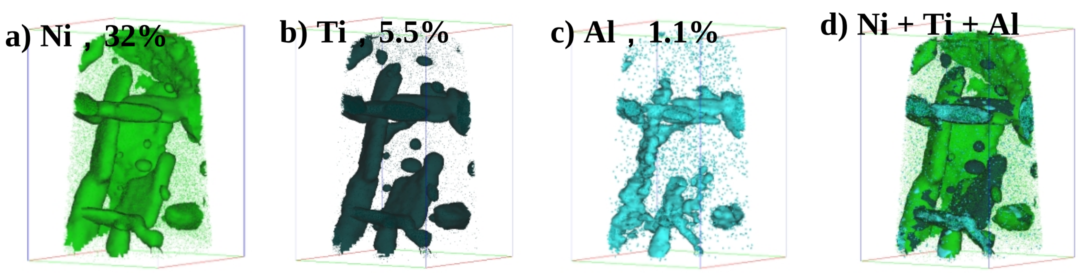

Fig. 9 Isoconcentration covers of Ni, Ti, and Al

Discussion

Strengthening mechanism. There are a large amount of alloy elements including Ni, Mo, Ti, and Al in T250 maraging aging steel. These alloy elements will dissolve into matrix to cause solid-solution strengthening during the solid-solution treatment, but most alloy elements will be precipitated in form of strengthening phase after aging. According to the test, there are rich contrasts and refined corrosive pits that is, high-density dislocation and second phases in diffuse distribution. As the size is in nm magnitude, so the particles cannot be observed in microstructure. Because of the precipitation of second phases, alloy elements dissolved in α-Fe greatly decreases, to make solid-solution strengthening effect weak. When martensite matrix is under external stress, the inhibition of the prior austenite crystal boundary against dislocation may be replaced with a large amount of substructures and lath boundaries with smaller interval [5, 6]. To sum up, aging treatment is the principal way to obtain ultra-high strength for T250 steel.

Phase exploration. In the spinning structure of T250 steel, there are a great amount of second phases in diffuse distribution in martensite lath boundary and lath. These second phases are composed of two parts, one exist since they cannot be dissolved in high-temperature solid solution, while the other precipitates during spinning. After aging, the phases changes. The structure of Ni_3Al intermetallic compounds is face-centered cubic, which are the same as the matrix, and the lattice constant is similar to that of matrix [7]. Moreover, because of low phase interface energy, Ni_3Al can be evenly precipitated in fine particles to inhibit dislocation and produce significant strengthening effect. According to EDS component analysis, Ni and Ti contents in matrix structure are relatively high, and Al can be hardened in T250 steel, so there are a large amount of $Ni_3(Al,Ti)$ phases, which has been verified in 3DAP test. With the rise of aging temperature, Ni_3Al compacts and grows, and Ti tends to be attached with cored Ni_3Al since it is saturated in matrix. Therefore, it shows that Ni_3Al gradually turns to $Ni_3(Al,Ti)$ in major morphology of strip-rod. Similarly, rod-shape Al_3Ti gradually turns to $Ni_3(Al,Ti)$ with the rise of temperature. Mo is an important strengthening element in T250 steel, which can increase the quenching degree of steel [8]. According to SEM and XRD results, there are large-particle residues in solid-solution sample, which are Fe_2Mo difficult to be dissolved, that is particles in (200~400) nm observed in SEM morphology. After aging, large particles gradually reduce. Fe_2Mo belongs to Laves phase which has a very good strengthening effect. However, Fe_2Mo also contains Si, which results from the affinity between Si and Mo [9]. Therefore, Fe_2Mo gradually turns to $MoSi_2$ with the rise of aging temperature.in diffuse distribution.

Conclusions

(1) The structure of spinning T250 sample turns to be tenuous and directional because of stress, and its matrix structure is martensite matrix with a great amount of $Ni_3(Al,Ti)$ in size of about (5-50) nm, a few of Fe_2Mo in size of about (200-400) nm, and other fine globular and rod phases, including phases Al_3Ti, $MoSi_2$, and Ni_3Al.

(2) The matrix structure of T250 steel is still martensite after spinning and aging, and the types of second phases keep constant, while the phases and particle morphology have change. With the rise of aging temperature, phases Al_3Ti and Ni_3Al turn to $Ni_3(Al,Ti)$, and Fe_2Mo to $MoSi_2$, and globular $Ni_3(Al,Ti)$ gradually combines and precipitates in strip-rod shape. After aging, the hardness improves mainly because of work hardening and aging strengthening.

References

[1] Decker R F, Eash J T, Goldman A J: Trans ASM Vol. 55 (1962), p. 58-76

[2] Zhongguo Liu, Jinghai Zhang: Bao Steel Technology (2007), p. 71-74 (In Chinese)

[3] Guang Chen, Yuqing Wen: J. Iron. Steel. Res. Vol. 5 (1993), p. 89-93 (In Chinese)

[4] Yunxing Zheng, Shoumou Xi: Hot Working Technology Vol. 37 (2008), p. 29-31 (In Chinese)

[5] Qiang Zhang, Mingjian Wang, Liwu Zhang, et al: Trans. Mater. Heat. Treat. Vol. 25 (2004), p 30-34 (In Chinese)

[6] Yi He, Ke Yang, Pingli Mao, et al: J. Aeronaut. Mater. Vol. 22 (2002), p. 1-5 (In Chinese)

[7] Xiaoming Wang, Zuchang Zhu: Heat Treatment Vol. 25 (2010), p. 6-11 (In Chinese)

[8] Golovin S A, Fomicheva N B, Morozyuk A A: Powder Metall. Met. Ceram. Vol. 32 (1993), p. 832-835

[9] Wei Sha: Iron and Steel Vol. 29 (1994), p. 47-51 (In Chinese)